

Dry etching techniques for active devices based on hexagonal boron nitride epilayers

Samuel Grenadier, Jing Li, Jingyu Lin, and Hongxing Jiang^{a)}

Department of Electrical and Computer Engineering, Texas Tech University, Lubbock, Texas 79409

(Received 19 April 2013; accepted 7 October 2013; published 22 October 2013)

Hexagonal boron nitride (hBN) has emerged as a fundamentally and technologically important material system owing to its unique physical properties including layered structure, wide energy bandgap, large optical absorption, and neutron capture cross section. As for any materials under development, it is necessary to establish device processing techniques to realize active devices based on hBN. The authors report on the advancements in dry etching techniques for active devices based on hBN epilayers via inductively coupled plasma (ICP). The effect of ICP radio frequency (RF) power on the etch rate and vertical side wall profile was studied. The etching depth and angle with respect to the surface were measured using atomic force microscopy showing that an etching rate $\sim 1.25 \mu\text{m}/\text{min}$ and etching angles $>80^\circ$ were obtained. Profilometer data and scanning electron microscope images confirmed these results. This work demonstrates that SF_6 is very suitable for etching hBN epilayers in RF plasma environments and can serve as a guide for future hBN device processing. © 2013 American Vacuum Society. [<http://dx.doi.org/10.1116/1.4826363>]

I. INTRODUCTION

Hexagonal BN is a wide band gap nitride semiconductor with an energy gap of about 6.1 eV. It is the least studied nitride semiconductor. Fundamentally, hBN has a hexagonal layered structure while other nitride semiconductors (AlN, GaN, and InN) are all wurtzite in structure, which makes hBN very unique and potentially suitable for many applications. Recent progresses have revealed that hBN is highly promising as an active material for deep UV (DUV) emitters and detectors.^{1–6} Moreover, due to its layered structure and nearly perfect lattice constant match to graphene, hBN is considered as the ideal template and gate dielectric layer in graphene electronics and optoelectronics.^{7,8} While detailed device fabrication processes including dry etching have been well established for other nitride semiconductors,⁹ the same cannot be said for hBN. With recent rapid development in material growth and fundamental understanding, development of the basic device processing techniques including dry etching is urgently needed to serve as a guide for the demonstration of active devices based on hBN and hBN/graphene heterostructures.

While much interest has been placed on hBN in DUV photonics and graphene applications, it is often overlooked that hBN also possesses extraordinary potential for solid-state neutron detector applications. This stems from the fact that the boron-10 (^{10}B) isotope has a capture cross-section of 3840 b for thermal neutrons with an energy of 25 meV. This is much larger than other isotopes. During the neutron capture process, the boron decays into lithium and alpha particles.¹⁰ These particles then generate electrons and holes in the semiconductor material. Epitaxial layers of hBN have been synthesized by metal-organic chemical vapor deposition (MOCVD)^{2–6} and utilized to investigate the potential of hBN for neutron detector applications.¹¹ To partially address

the key requirement of long carrier lifetime and diffusion length for solid-state detectors, microstrip metal–semiconductor–metal (MSM) detectors were fabricated and tested.¹¹ Reactor testing with continuous irradiation from a thermal neutron beam generated an appreciable current response in hBN detectors. Much improvement can be anticipated with improved device architectures and processing techniques. In particular, it is expected that optimizing the microstrip etching profile with deeper trenches will allow more effective utilization of the excellent lateral transport properties of layered hBN and enhanced device performance, particularly as material thickness is increased. Our initial results showed that using a Cl based plasma did indeed etch our hBN. However, etching rate and profile were both quickly becoming limiting factors in attainable etch depth even after etch optimization.

In this work, we focus on establishing and optimizing the inductively coupled plasma (ICP) dry etching process of hBN epitaxial layers grown by MOCVD, by adopting basic processes from GaN.⁹ Material thickness and etching depth are some of the most important parameters in the detector device performance, particularly because the absorption length of thermal neutrons in hBN is long ($\sim 50 \mu\text{m}$ for ^{10}B enriched hBN) and the carrier diffusion length is comparably short. While the previously established methods for III-nitrides do indeed etch hBN, the etching rate and profile are both unsuitable for the needs of practical devices. The side wall etching profile was quickly becoming a limiting factor in etching depth. Furthermore, achieving the vertical sidewall etching profile will be very important if utilizing hBN for other active photonic and electronic device applications including waveguides, light emitting diodes, strip lasers, and heterojunction devices.

The etching rate for GaN in Cl_2 plasma at a RF 1 power of 300 W is measured to be around $1 \mu\text{m}/\text{min}$ while the etching rate of hBN in Cl_2 is measured to be only around $250 \text{ nm}/\text{min}$ with a depth limiting profile. This led us to try new plasma chemistries. We chose to substitute the

^{a)}Electronic mail: hx.jiang@ttu.edu

established Cl-plasma chemistry from GaN and AlN with SF₆, a chemistry frequently used for the etching of silicon. Fluorine plasmas have so far shown some of the highest etching rates for boron films.¹² Most notably, recent work has been done on the dry etching of enriched boron in pillar structure neutron detectors using SF₆ plasma.¹² We also found reports on the cleaning of boron from the walls of monuclear fusion reactor chambers using H-, Cl-, and F-based plasmas.^{13–15} However, while some plasma etching processes for boron films have been explored, dry etching of high quality epitaxial hBN films has yet to be studied.

II. EXPERIMENT

To test our approach, hBN epitaxial layers with thickness between 1 and 4 μm were synthesized by MOCVD using natural triethylboron (TEB) and ammonia (NH₃) as B and N precursors, respectively. These epilayers were grown on sapphire substrates using a low temperature (800 °C) buffer layer of BN. X-ray diffraction (XRD) and photoluminescence (PL) data from these epilayers indicate that these are indeed hexagonal in phase and are of high quality. The XRD rocking curve of the hBN (0002) diffraction peak has a full width at half maximum (FWHM) of ~380 arc sec, which is comparable to those of GaN epilayers with a similar thickness. These results have already been discussed in previous works from our group.^{2–6} In order to test with a similar device structure to that of our previous MSM detectors,¹¹ we fabricated strips with widths ranging from 8 to 12 μm on hBN epilayers. The hBN was coated with SPR-220 photoresist (4.5 μm in thickness). Deep UV photolithography used to ensure resolution was maintained through smaller device feature sizes. ICP etching was achieved with the Plasmatherm 790 ICP machine.

Our results showed that in varying ICP RF 1 power, the etching rate and etching profile could be greatly improved. RF2 and ICP chamber pressure were held constant at 150 W and 6 mTorr, respectively, and showed little impact on etch profile when changed. Substrate temperature was not recorded.

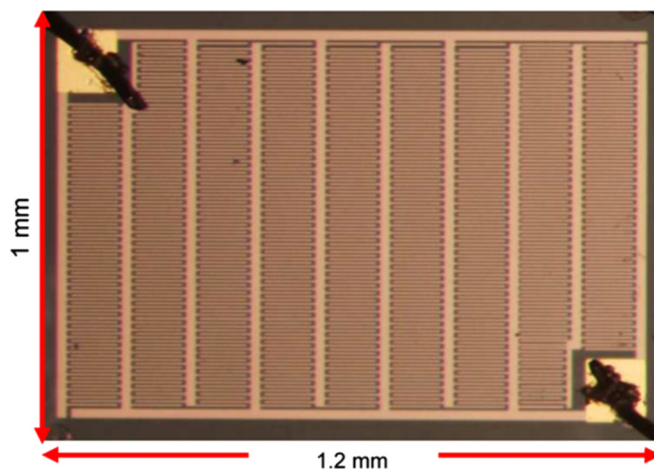


Fig. 1. (Color online) Optical image showing the MSM UV and neutron detector layout.

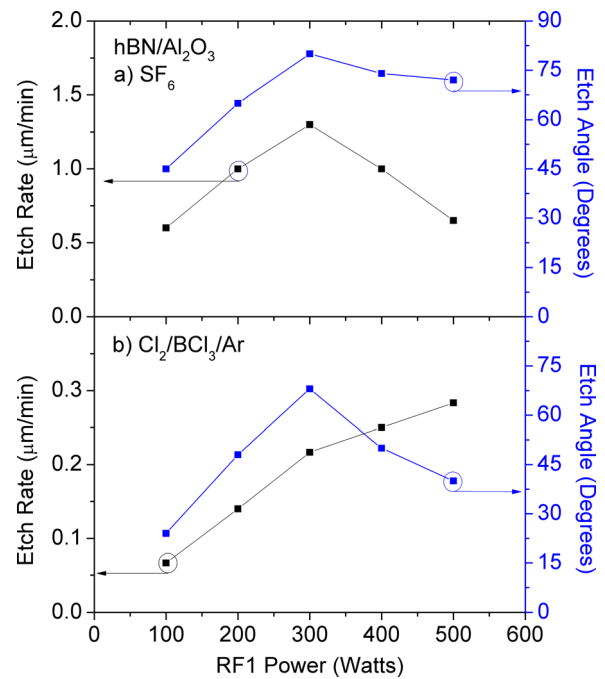


Fig. 2. (Color online) RF1 power dependence for hBN epilayers etched in (a) SF₆ and (b) Cl₂/BCl₃/Ar plasma.

III. RESULTS AND DISCUSSION

Figure 1 shows an optical microscope image of a fabricated MSM detector. Figure 2(a) shows the measured etching rate and side wall angle with respect to the surface as functions of the RF1 power for hBN epilayers in a plasma chemistry of 5 sccm SF₆. Figure 2(b) shows the measured etching rate and angle of hBN as functions of the RF1 power in a plasma chemistry consisting of Cl₂, BCl₃, and Ar with flow rates of 16, 5, and 4 sccm, respectively. We observed the optimal etching condition with sharpest profile and highest etching rate at RF1 power set to 300 W in both plasma chemistries. The results were measured using atomic force microscopy (AFM). Figure 3 shows an AFM profile of one wall of the hBN strip. SEM images were taken from some samples to ensure that the probe based results were indeed accurate. Our results clearly demonstrate that a higher etching rate was achieved with the use of SF₆. An increase in etching rate of as much as 5× that of Cl₂ and an

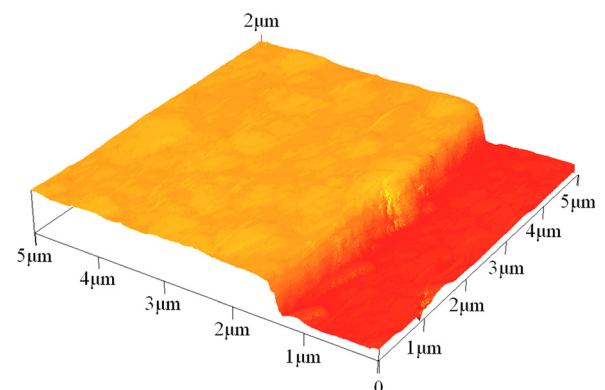
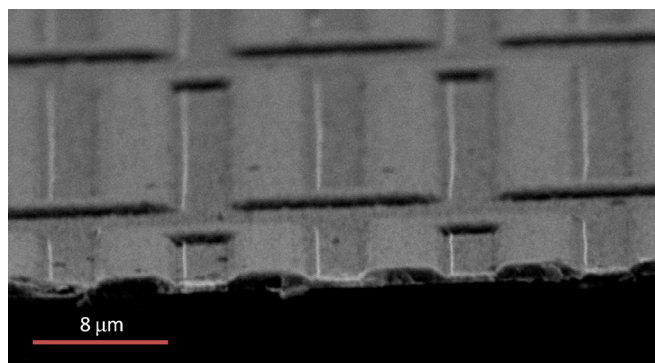
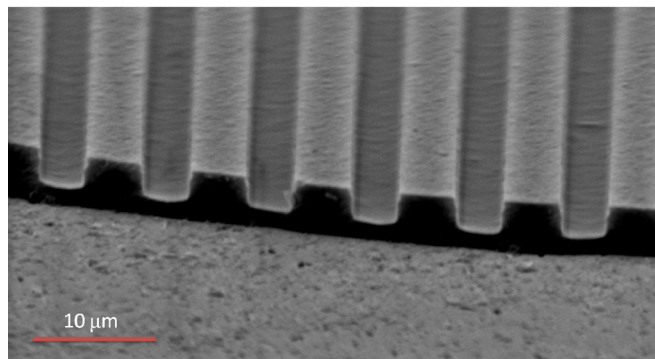


Fig. 3. (Color online) AFM profile of hBN strip etched in SF₆.



(a)



(b)

FIG. 4. (Color online) SEM image of the cross-section profile of hBN strip devices etched in (a) Cl_2 and (b) SF_6 for comparison.

improvement in profile from $\sim 70^\circ$ to $> 80^\circ$ was seen. Shown in Fig. 4 is a comparison between strips etched in Cl_2 and SF_6 . Etch depths $> 3.5 \mu\text{m}$ are now achievable in just one photoresist deposition while still maintaining an excellent vertical etching profile using SF_6 . This is a vast improvement over the profile seen in Fig. 4(a), which was etched in Cl_2 .

In our ICP, RF1 controls plasma ion energy, while RF2 controls ion density. Results from etching with Cl_2 showed that RF2 has little to no effect on the etching profile. This is because ion density only has effects on etching rate and polymer deposition as seen in silicon etching performed by ICP.¹⁶ As such, we decided to push aside RF2 as an important parameter once the profile achieved its maximum and we had an appropriate etching rate.

SF_6 even when used in etching of other III-nitride materials does not normally show etching rates approaching this magnitude with materials like AlN showing etching rates of $\sim 180 \text{ nm/min}$.¹⁷ This remarkable etching rate is likely due to the strong interaction between fluorine and boron creating highly volatile BF_3 ,¹⁸ whereas Cl-based environments produce BCl_3 which has a low vapor pressure and may be easily redeposited.

IV. SUMMARY AND CONCLUSIONS

To summarize, we have demonstrated an effective dry-etching approach for hBN device fabrication using SF_6 based ICP. By optimizing the etching parameters, we are able to achieve an etching rate $\sim 1.25 \mu\text{m/min}$ and profile angle $> 80^\circ$. Further understanding is needed on the passive by-products that may be produced during this etching process. In the future, we would like to analyze the effects of the introduction of an inert gas like Ar to the plasma would have to further control and improve etching characteristics. Even so, ICP with a SF_6 plasma chemistry provides a technique for effective fabrication of hBN devices including deep UV optoelectronic devices, neutron detectors, and hBN/graphene based heterostructure devices.

ACKNOWLEDGMENTS

This work was supported by DHS ARI program entitled “ARI-MA: Collaborative research: Hexagonal boron nitride based neutron detectors” (2011-DN-077-ARI048). Jiang and Lin are grateful to the AT&T Foundation for the support of Ed Whitacre and Linda Whitacre endowed Chairs.

- ¹K. Watanabe, T. Taniguchi, and H. Kanda, *Nature Photonics*, **3**, 591 (2009).
- ²R. Dahal, J. Li, S. Majety, B. N. Pantha, X. K. Cao, J. Y. Lin, and H. X. Jiang, *Appl. Phys. Lett.* **98**, 211110 (2011).
- ³S. Majety, J. Li, X. K. Cao, R. Dahal, B. N. Pantha, J. Y. Lin, and H. X. Jiang, *Appl. Phys. Lett.* **100**, 061121 (2012).
- ⁴B. Huang, X. K. Cao, H. X. Jiang, J. Y. Lin, and S. H. Wei, *Phys. Rev. B* **86**, 155202 (2012).
- ⁵S. Majety, X. K. Cao, J. Li, R. Dahal, J. Y. Lin and H. X. Jiang, *Appl. Phys. Lett.* **101**, 051110 (2012).
- ⁶J. Li, S. Majety, R. Dahal, W. P. Zhao, J. Y. Lin, and H. X. Jiang, *Appl. Phys. Lett.* **101**, 171112 (2012).
- ⁷N. Alem, R. Erni, C. Kisielowski, M. D. Rossell, W. Gannett, and A. Zettl, *Phys. Rev. B* **80**, 155425 (2009).
- ⁸R. V. Gorbachev *et al.*, *Small* **7**, 465 (2011).
- ⁹S. J. Pearton, J. C. Zolper, R. J. Shul, and F. Ren, *J. Appl. Phys.* **86**, 1 (1999).
- ¹⁰R. F. Barth, A. H. Soloway, and R. G. Fairchild, *Sci. Am.* **263**, 100 (1990).
- ¹¹J. Li, R. Dahal, S. Majety, J. Y. Lin, and H. X. Jiang, *Nucl. Instrum. Methods Phys. Res. A* **654**, 417 (2011).
- ¹²L. F. Voss, C. E. Reinhardt, R. T. Graff, A. M. Conway, R. J. Nikolić, N. Deo, and C. L. Cheung, *J. Electron. Mater.* **39**, 263 (2010).
- ¹³H. Toyoda, T. Isozumi, H. Sugai, and T. Okuda, *J. Nucl. Mater.* **162**, 732 (1989).
- ¹⁴H. Toyoda, A. Hanami, M. Yamage, and H. Sugai, *Jpn. J. Appl. Phys.* **30**, L514 (1991).
- ¹⁵H. Toyoda, A. Hanami, and H. Sugai, *Jpn. J. Appl. Phys., Part 1* **29**, 1322 (1990).
- ¹⁶L. Sun and A. Sarangan, *J. Micro/Nanolith. MEMS MOEMS*, **10**, 023006 (2011).
- ¹⁷D. Chen, D. Xu, J. Wang, B. Zhao, and Y. Zhang, *Vacuum* **83**, 282 (2008).
- ¹⁸L. F. Voss, C. E. Reinhardt, R. T. Graff, A. M. Conway, R. J. Nikolić, N. Deo, and C. L. Cheung, *Nucl. Instrum. Methods Phys. Res. A* **606**, 821 (2009).